Femtosecond measurements of the time of flight of photons in a three-dimensional photonic crystal

Yu. A. Vlasov,* S. Petit, G. Klein, B. Hönerlage, and Ch. Hirlimann
Institut de Physique et Chimie des Materiaux de Strasbourg, Groupe d'Optique Non Lineaire et d'Optoelectronique, UMR 4075 CNRS-ULP 23, rue du Loess, 67037 Strasbourg Cedex, France
(Received 28 January 1999)

We report on experimental measurements of the propagation behavior of short optical pulses in a three-dimensional photonic crystal in the visible spectrum. The propagation delay of 70 fs light pulses transmitted through a sample of a fcc synthetic opal at frequencies lying in a photonic stop band was measured directly using a time-of-flight technique. Taking into account spectral reshaping of the transmitted pulses as well as the residual frequency chirp of the incoming pulses, it is found that the pulses significantly slow down at the photonic band edges. [S1063-651X(99)06807-5]

PACS number(s): 42.70.Qs, 42.65.Re, 78.47.+p

I. INTRODUCTION

There has been much recent interest in the fabrication and study of spatially periodic dielectric structures with a periodicity matching the wavelength of electromagnetic (em) waves in the visible range [1]. Spatial modulation of the refractive index leads to an imaginary value for the wave vector in certain frequency ranges, called photonic stop bands—that is, to an exponential decay of em waves within the medium and to a high reflectivity due to the constructive Bragg interference. As for the electrons in solids, a photonic band structure develops for photons propagating in such *photonic crystals*. Under favorable conditions the density of photonic states (DOS) in photonic crystals can be significantly depleted or even suppressed to zero, giving rise to photonic band gaps (PBG's) [1]. At the edges of the photonic stop bands the photon dispersion curve strongly deviates from a linear behavior and exhibits pronounced bending. Such heavy photons were shown to possess an increased DOS, high local em fields, and small group velocity [2–4]. These unusual properties of heavy photons can lead to an increase of the rate of the spontaneous-emission process [2], to an enhancement of optical gain [3], to a more efficient nonlinear optical response [4], etc. Experimental studies of the dispersion of heavy photons are, however, scarce and incomplete. Studies of the light propagation in a one-dimensional (1D) periodic structure allowed us to propose a photonic delay line [5]. Photon dispersion curves in a 2D photonic crystal were studied using a coherent microwave transient technique [6], while, to date, the measurements of photon dispersion relation at the band edges in 3D photonic crystals have been limited to the case of an ordered colloid crystal [7] and performed using a modified Mach-Zehnder interferometer.

In this paper we present time-of-flight measurements aimed at the determination of the photon dispersion in a three-dimensional (3D) photonic crystal: synthetic opal [8–15]. It is known that synthetic opals, made of submicrometer silica spheres, closely packed in a face centered cubic (fcc) lattice with a period of about 200 nm, possess photonic stop bands throughout the visible spectrum [8,9]. It has been further shown that, by varying the photonic lattice parameters of opals (refractive index contrast and volume packing fraction of the spheres β), it should be possible to achieve a small but complete photonic band gap extending throughout the Brilloiun zone [10,11]. These predictions stimulate intense experimental studies for various routes to fabricating so-called ''inverted opals,'' where the refractive index of the interstitial volumes is larger than that of the spheres. The silica periodic opal lattice is used as a scaffolding for high refractive index materials like titanium oxide [12], graphite [13], or semiconductor quantum dots [14]. After removing the silica spheres from the structure the refractive index contrast can be increased to extremely high values, sufficient for opening up a complete photonic band gap. Even for an inverted opal with a not as high refractive index contrast of only 2, an enhancement of optical gain by a factor of 3 and the appearance of a laser effect were reported recently [15], and this is supposed to be due to the bending of the photon dispersion curve at the edges of the stop band. In view of all these achievements, the determination of the transport properties and the photon dispersion relation in opals become increasingly important.

The paper is organized as follows. In Sec. II we briefly mention the sample preparation and characterization. Then we describe the experimental setup and procedure. In Sec. III we present the results of time-of-flight measurements. Sec. IV is devoted to a discussion of the phase and frequency distortion of the probe pulses and corresponding corrections to raw experimental data. Finally we qualitatively discuss the two main mechanisms, which can contribute to an observed significant increase of delay times at the edges of the photonic stop band, namely, the anomalous group velocity dispersion and light localization.

II. EXPERIMENT

The samples of synthetic opals used in this study were fabricated through several technological stages: the synthesis

*On leave from A. F. Ioffe Physical Technical Institute, Polytechnicheskaya 26, St. Petersburg, Russia. Present address: NEC Research Institute, 4 Independence Way, Princeton, NJ 08540. URL: www.neci.nj.nec.com/homepages/vlasov

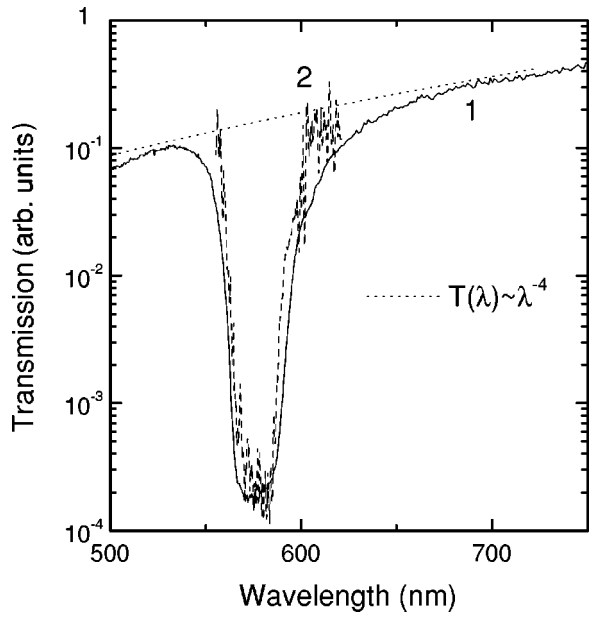

FIG. 1. Transmission spectra for incidence normal to (111) plane of the opal sample of 370-μm thickness. Spectrum 1 is obtained using the collimated light from an incandescent lamp. Spectrum 2 is the transmission of the full femtosecond continuum as described in the text.

of monodisperse colloidal silica spheres [16], the sedimentation of the suspension to an ordered solid ceramics, and the subsequent sintering to enhance hardness. In this way, the sample, composed of spheres (refractive index $n_a = 1.37$), having a mean diameter $D = 254$ nm (standard deviation δ less than 5%) and a volume packing fraction of $\beta = 0.76$ (fcc lattice constant $a = 340$ nm) was prepared. The sample was mechanically polished down to a platelet having a 370 ± 20-μm thickness and 6×8-mm lateral dimensions with a base surface corresponding to a (111) plane of the fcc lattice. In order to decrease incoherent scattering on the surfaces, the sample was immersed in glycerol, thus implying that the refractive index of the voids between the silica spheres was $n_b = 1.475$.

To probe the transmission spectra of the opal sample, we used the technique proposed in Ref. [10]. The sample was illuminated at an incidence normal to a (111) plane with a highly collimated white-light beam from an incandescent lamp through a 100-μm aperture placed immediately in front of the sample, thus defining the probing area. Only the zero-order transmitted beam is collected. Thus a nearly plane wave geometry is achieved for the transmission measurements. The spectra are recorded with a double monochromator having a 1-nm spectral resolution. Figure 1 presents the thus obtained transmission spectrum 1 exhibiting a photonic stop band dip at 575 nm. This dip is accompanied by an intense line in the reflection spectrum, with the reflectivity close to unity, which repeats the shape and spectral position of the dip in transmission [8–10]. A smooth decline in the transmission spectra to shorter wavelengths is attributed to Rayleigh scattering [10] from the surfaces and from lattice defects. In the long-wavelength region this tail can be fitted by the characteristic dependence $T \propto \lambda^4$ (see dotted line in Fig. 1). The attenuation length due to coherent Bragg diffraction at the center of the stop band can be estimated as 57 μm or 230 lattice planes in the (111) direction, in accordance with the results of Ref. [10] obtained with an analogous sample.

For time-of-flight measurements we used a typical setup for a background-free correlation based on a dispersion compensated colliding pulse mode locked (CPM) laser oscillator [17] generating light pulses of 70-fs duration centered at a wavelength of 630 nm. The pulses were amplified up to 1 J using a multipass dye amplifier [18] pumped by a frequency doubled Nd: YLF Q-switched laser operated at a 1-kHz repetition rate. The generation of tunable pulses was achieved by first coupling part of the amplified pulse beam into a 7-mm-long, polarization preserving, optical silica fiber, in order to generate a broad continuum spectrum. After collimation of the light at the exit of the fiber, the continuum beam crossed a dual pass SF11 glass prism compressor, and part of the spectrum was selected by placing an adjustable slit in the space region where the spectrum was dispersed [19]. A careful setting of the slit width allowed a compressing of the probe pulses back to a 70-fs duration with a central wavelength tunable from 530 nm to 650 nm spanning over the entire width of the photonic stop band. The probe pulses were frequency mixed with the 630-nm pump pulses in a phase-matched, 200-μm-thick, KDP crystal, and the intensity of the summed frequency light was measured as a function of the time delay between the pump and the probe. This time delay was adjusted by means of a translation stage with a 0.1-μm mechanical resolution (0.6-fs time delay resolution). In order to increase the signal-to-noise ratio the probe beam was amplitude modulated by means of a mechanical chopper operated at 80 Hz, and the signal, collected by a photomultiplier, was amplified by a lock-in amplifier. The spectra of the probe pulses before and after the sample were analyzed using a 25-cm focal length spectrometer and an optical multichannel analyzer.

The time-of-flight experiments were performed by introducing the sample into the probe beam of the correlator and by measuring the change in time delay t and width of the cross-correlation traces as a function of the central wavelength of the probe beam. The base (111) face of the opal sample was oriented to be perpendicular to the probe beam. The zero time delay t_0 was determined for each wavelength by taking the sample out of the beam and recording a reference cross-correlation trace. In order to select small homogeneous regions of the sample, the probe beam was focused down on the sample, and then, after transmission, was collimated back using 10-cm focusing lenses. The exact position of the laser spot on the sample surface during measurements was carefully controlled with a microscope. The solid angle of the beam between the small aperture lenses was less than 0.5 degree.

III. RESULTS

In general, different wave vectors are probed for different angles and, therefore, such geometry can in principle lead to serious errors in a group velocity dispersion determination. In order to check that we measured the transmission spectrum (spectrum 2 in Fig. 1) at the output of the correlator setup using the same 70-fs broadband continuum, which is used for generation of the tunable femtosecond pulses. Com-

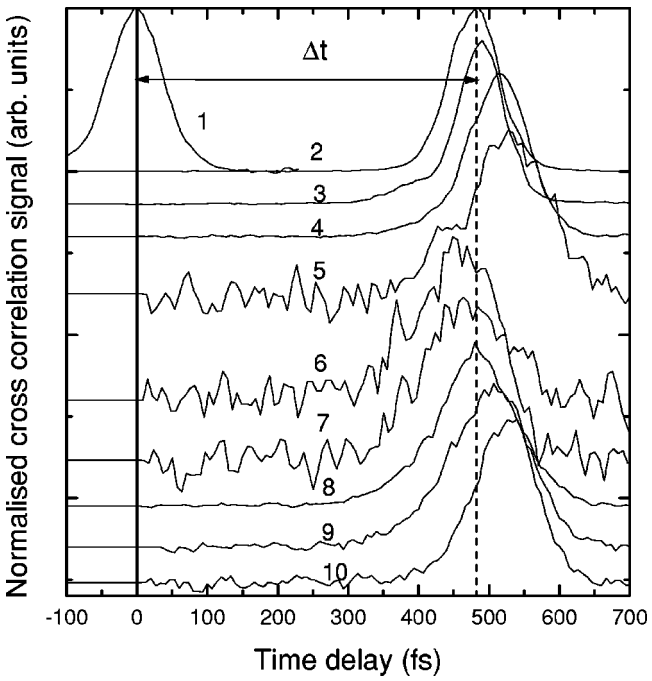

FIG. 2. Cross-correlation traces for transmitted pulses as a function of the central wavelength of incoming pulse: 2, 640 nm; 3, 610 nm; 4, 591 nm; 5, 580 nm; 6, 572 nm; 7, 559 nm; 8, 557 nm; 9, 554 nm; 10, 550 nm. Trace 1 is a cross-correlation signal without the sample for a 640-nm central wavelength of the pulse.

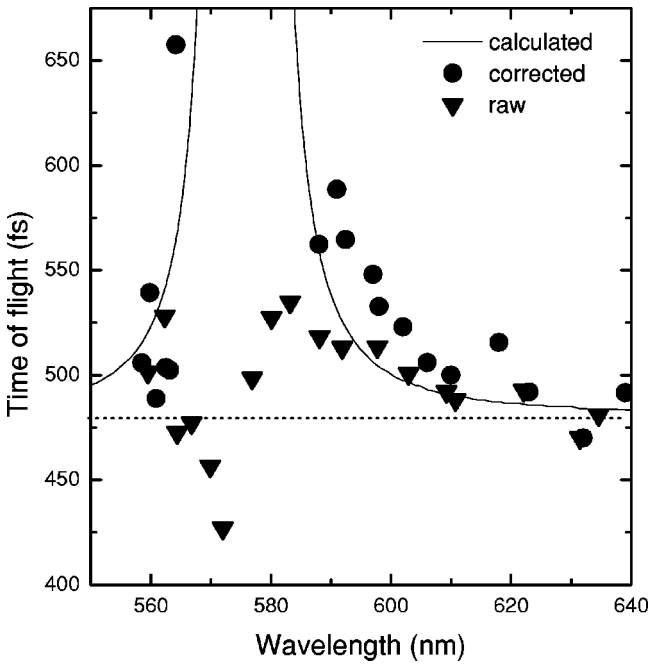

FIG. 3. Measurement of the time delay experienced by 70-fs light pulses crossing a 370-μm-thick opal sample along the $\langle 111 \rangle$ direction, in the vicinity of a stop band (dots). Filled circles represent the experimental results corrected for the phase and frequency distortion of the incoming pulses as described in the text. The time delays are compared to theoretical calculations (triangles) made according to the model proposed in Ref. [24].

parison with spectrum 1, obtained in a nearly plane-wave geometry, showed that our correlator does not introduce significant additional distortion to the wave front.

Figure 2 represents the cross-correlation traces measured as a function of the wavelength of the probe pulse. It is seen that the light pulses delay and broaden when their central wavelength approaches the center of the stop band (see traces 1–5). The attenuation of the pulses also becomes very strong in the stop-band region. Due to the limited dynamic resolution of the setup we were unable to detect pulses with wavelengths very close to the center of the stop band. However for pulses in the immediate vicinity of the stop-band center (see traces 6 and 7 in Fig. 2) the maximums of the pulses arrive earlier than that for pulses at the red side of the stop band (see trace 1). The time of flight $\Delta t = t - t_0$ can be measured as a time interval between the arrival of the pulse maximum transmitted through the sample and the maximum of the reference pulse. This time of flight Δt is plotted in Fig. 3 (triangles) as a function of the central wavelength of the incident pulse. In the long-wavelength limit the propagation of pulses through a periodic structure should be well described by an effective dielectric constant n_{eff} of the media. Taking into account the parameters of the opal photonic lattice, n_{eff} can be estimated as 1.39, using the Maxwell-Garnett approximation [20]. This value implies a group delay $\Delta t = d/c(n_{eff} - 1)$ (where c is the vacuum speed of light and d the sample thickness) of about 481 fs, very close to our experimentally observed value of 490 fs at a wavelength of 640 nm far to the red of the long wavelength edge of the stop band. It is seen from Fig. 3 that, starting from this value, the time Δt increases to about 530 fs at the long-wavelength photonic band edge at 590 nm and then suddenly falls down to 420 fs at the stop-band center with a subsequent increase to 530 fs at the short-wavelength edge. If we assume that the propagation of pulses within the stop band can also be described by the group velocity V_g, then we have a decrease of V_g to $0.9c/n_{eff}$ at the band edges and a superluminal velocity of $1.15c/n_{eff}$ at the midgap.

IV. WAVELENGTH AND TIME DELAY CORRECTIONS TO THE EXPERIMENTAL DATA

A. Wavelength corrections

Recently several groups reported superluminal tunneling times of photons through a dielectric multilayer stack (1D photonic crystal) at the midgap frequencies [21,22]. It has been shown that this observation does not conflict with causality because of the strong attenuation suffered by transmitted signals. Indeed, within the photonic stop band the wave vector k becomes purely imaginary due to destructive Bragg interference. Since the transmitting pulse decays faster than it propagates, the concept of the group velocity becomes meaningless. It was shown that the propagation of pulses in this case is better described by the energy velocity, defined as a ratio of the Poynting flux S and electromagnetic energy density.

Although it seems reasonable to interpret our results in this context, we believe, however, that it is the distortion of the spectral shape of our pulses, that should first be taken into account. Despite the fact that the spectral width of the nearly Fourier-limited 70-fs pulses (10 nm) is smaller than the width of the photonic stop band (45 nm), the spectral shape of the pulses is strongly distorted. Figure 4(A) represents spectra of the incident and transmitted pulse tuned to

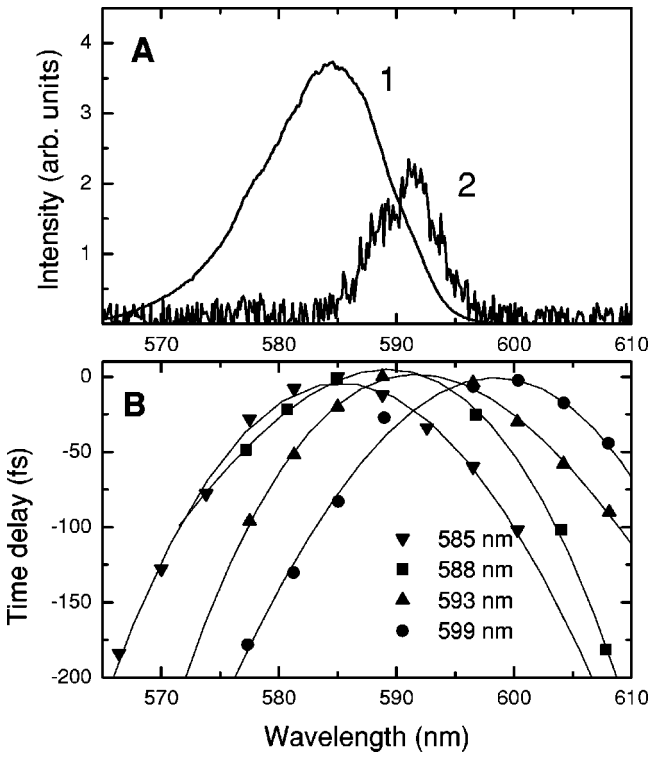

FIG. 4. (A) Spectra of the incoming (1) and outgoing (2) pulses tuned close to the stop-band center. (B) Plot of the residual frequency chirp distorting the phase distribution of the incoming pulses for a set of central wavelengths of the pulses. The experimental setup is such that the central wavelength acts as a time reference. As can be seen, the far spectral wings of the pulses experience strong third-order phase distortions.

584 nm. It can be clearly seen that the central part and short-wavelength wing of the pulse are ''eaten out,'' while the long-wavelength wing can still be measured. It is just this part of the propagated pulse, that is detected by the cross-correlation technique, because the dynamic resolution of our correlator is limited to three orders of magnitude. This outgoing pulse has a spectral width of only 5.5 nm corresponding to a time duration of as much as 250 fs. This spectral-temporal change is of great importance when looking for non-linear optical propagation. In our linear situation it is clear that the raw experimental data plotted in Fig. 3 have to be corrected taking into account this spectral reshaping. For example for the incoming pulse shown in Fig. 4(A) with a center at 583 nm, the corresponding outgoing transmitted pulse is centered at 590 nm. Therefore the time of flight measured with such a pulse corresponds to a 590-nm wavelength rather than to a 583-nm one. We performed analogous measurements of the spectra of transmitted pulses each time the cross-correlation traces were measured. Using these data the spectral corrections to the central wavelength of the probe pulses (x axis in Fig. 3) were made.

B. Time delay corrections

As is known, the glass prism optical compressors introduce third-order phase distortions in light pulses [23]. This higher order frequency chirp is more pronounced on the far wings of the pulse spectrum than at its center. This is of primary importance in our experiment, as a strong spectral reshaping takes place during the propagation of light that shifts the central wavelength of the pulses to the far wings of the spectrum. Therefore the time delay of the raw experimental data (y axis in Fig. 3) must also be corrected by adding the initial chirp-induced time delay, which corresponds to the corrected central wavelength of the transmitted pulse. For this purpose the frequency chirp of the tunable 70-fs pulses was carefully measured. For a given tuned probe pulse, the prism compressor was adjusted in such a way as to give the shortest possible duration, as determined by a frequency up-conversion cross-correlation measurement with the unperturbed pulse as a reference. The up-converted signal was then spectrally analyzed by means of a spectrometer and a photomultiplier, and the time delay of the frequency components was recorded [23]. A meaningful series of such measurements is shown on Fig. 4(B) for probe pulses at 585, 588, 593, and 599 nm. For each central wavelength a quadratic fit could be performed on the data, demonstrating the cubic nature of the phase distortion left in the pulses. As can be seen, time delays as large as 200 fs were recorded on the far spectral wings of the pulses.

V. DISCUSSION

According to our previous discussions the raw experimental data shown in Fig. 3 as triangles have to be corrected in two ways. First the data must be plotted as a function of the transmitted central wavelength to account for spectral reshaping; second the raw measured time delays must be rescaled according to the chirp-induced delay in the incoming pulses. The resulting corrected time of flight Δt is plotted in Fig. 3 (filled circles) as a function of the corrected central wavelength of the transmitted pulse. It can be seen that the superluminal behavior characteristic of the raw experimental dependence is nothing but an artifact caused by a spectral reshaping of the pulses. At the same time it also can be seen that the corrected data still exhibit a considerable increase in time delays at the edges of the stop band. Note that the pulses tuned to the longer wavelength far from the stop band (larger than 600 nm) are practically unaffected by the latter, so that the corresponding time delays can serve as a good unperturbed reference. Taking this into account, it is seen that the pulses at the band edges are delayed for as long as 100–150 fs [slowed down to $(0.7–0.8)c/n_{eff}$].

In general, the time of propagation of photons in inhomogeneous media can be affected by various mechanisms. First it is natural to suppose that it is the anomalous photonic dispersion in periodic structure, that causes the observed delay. We calculate the dispersion relation for photons $k(\omega)$ propagating in the opal photonic lattice along the (111) direction using the analytical model proposed in Ref. [24]. Even though this model is based on a simple one-dimensional approach in a scalar wave approximation, it gives, nevertheless, qualitatively correct results for the dispersion at high-symmetry points, such as X and, especially, L in a fcc Brillouin zone, where a single lattice scattering component dominates. The time delay $\Delta t = d/V_g(\omega)$, where $V_g(\omega) = d\omega/dk(\omega)$, calculated for the point L of a fcc photonic Brillouin zone of a crystal with parameters of our opal sample is also plotted in Fig. 3. It can be seen that at both edges of the stop band the calculated group delays become

increasingly large due to a slowing down of the group velocity V_g. A reasonable agreement is observed between the experimental and calculated dispersion variations, especially taking into account the fact that there is no fitting parameter involved in the numerical calculations.

The above-mentioned mechanism based on anomalous group velocity dispersion is not the only one possible. Numerous papers on photon propagation in disordered media have shown that multiple scattering events can also significantly increase the dwell time of a photon inside the media [25,26]. Different paths of photons randomly scattered inside the media result in the appearance of a long-time exponential tail in the time-of-flight response [26], which reflects the distribution of dwell times. In the case of strong light scattering this tail can extend to time dealys as long as several milliseconds [27]. Recently it was pointed out that the propagation of light in opal-based photonic crystals is also strongly affected by incoherent scattering on numerous intrinsic defects of the opal fcc lattice [28]. Let us consider only one type of defect, which is an unavoidable source of disorder in opal-like self-organized photonic lattices—the deviation δ of the sphere's diameter, which in the case under consideration was measured to be about 5%. This corresponds to the same value of deviation of the lattice constant $a=D\sqrt{2}$. This value, being compared with the calculated normalized width of the (111) stop band $\Delta\lambda/\lambda_0$ in an ideal defect-free opal photonic lattice, can be the measure of the influence of disorder on the transport properties of photonic crystals [28]. For the present case, as is seen from calculations presented in Fig. 3, the $\Delta\lambda/\lambda_0$ is smaller than 1%. This means that local fluctuations of the photonic band edges are larger than the band gap width itself. It has been shown [28] that a situation with $\delta>\Delta\lambda/\lambda_0$ corresponds to a special regime of strong light localization. This regime is intermediate between the light localization in strongly scattering disordered media [25–27] and the localization of coherent Bloch states at the edges of a photonic gap in periodic photonic crystals [29]. These localized states are characterized by a huge enhancement of the light amplitude inside the structure and a corresponding increase in the lifetime, defined by large Q factors [28]. In our experiment a volume of the sample, large compared to the volume of the crystal unit cell, is probed and, therefore, large local fluctuations are averaged out and a smooth transmission curve and time-of-flight dependence are measured. It seems then that a slow percolation of photons between such localized states could also be a possible explanation of the observed dispersion behavior. Such tunneling should result in the appearance of long exponential tails in the time-of-flight response. We do observe the broadening of the transmitted pulses tuned to the center of the stop band. The limited dynamical resolution of our experimental setup does not allow, however, the study of this effect in detail. Further experimental and theoretical studies are necessary to identify the relative contributions of group velocity dispersion and photon localization to the observed pattern.

VI. CONCLUSIONS

In conclusion, femtosecond time-of-flight measurements were performed on a three-dimensional photonic crystal in the visible region of the spectrum. It is found that at the edges of a photonic stop band optical pulses are significantly slowed down. We obtain a good qualitative agreement between our experimental results and numerical calculations of the group velocity dispersion in opal photonic crystals. An analysis of the time-of-flight response indicates that the time delays are affected by the presence of defects in the photonic lattice of opals. Further insight into the possible role played by a strong light localization, which is expected at the edges of the photonic stop band, depends upon an improvement of the dynamical resolution of our experimental setup.

ACKNOWLEDGMENTS

Helpful discussions with E.L. Ivchenko and A.V. Selkin are gratefully acknowledged.

[1] For a recent review, see articles in, *Photonic Band Gap Materials*, edited by C. M. Soukoulis (Kluwer, Dordrecht, 1996).
[2] T. Suzuki and P. K. L. Yu, J. Opt. Soc. Am. B **12**, 570 (1995); M. D. Tocci, M. Scalora, M. J. Bloemer, J. P. Dowling, and C. M. Bowden, Phys. Rev. A **53**, 2799 (1996).
[3] J. P. Dowling, M. Scalora, M. J. Bloemer, and C. W. Bowden, J. Appl. Phys. **75**, 1896 (1994).
[4] M. Scalora, J. P. Dowling, C. W. Bowden, and M. J. Bloemer, Phys. Rev. Lett. **73**, 1368 (1994); J. Martorell, R. Vilaseca, and R. Corbalan, Appl. Phys. Lett. **70**, 702 (1997).
[5] M. Scalora, R. J. Flynn, S. B. Reinhardt, R. L. Fork, M. J. Bloemer, M. D. Tocci, C. M. Bowden, H. S. Ledbetter, J. M. Bendickson, J. P. Dowling, and R. P. Leavitt, Phys. Rev. E **54**, R1078 (1996).
[6] S. Y. Lin and G. Arjavalingam, Opt. Lett. **18**, 1666 (1993).
[7] I. I. Tarhan, M. P. Zinkin, and G. H. Watson, Opt. Lett. **20**, 1571 (1995).
[8] V. N. Astratov, V. N. Bogomolov, A. A. Kaplyanskii, A. V. Prokofiev, L. A. Samoilovich, S. M. Samoilovich, and Yu. A. Vlasov, Nuovo Cimento D **17**, 1349 (1995).
[9] V. N. Astratov, Yu. A. Vlasov, O. Z. Karimov, A. A. Kaplyanskii, Yu. G. Musikhin, N. A. Bert, V. N. Bogomolov, and A. V. Prokofiev, Phys. Lett. A **222**, 349 (1996).
[10] Yu. A. Vlasov, V. N. Astratov, O. Z. Karimov, A. A. Kaplyanskii, V. N. Bogomolov, and A. V. Prokofiev, Phys. Rev. B **55**, 13 357 (1997).
[11] K. Busch and S. John, Phys. Rev. E **58**, 3896 (1998).
[12] J. Wijnhoven and W. L. Vos, Science **281**, 802 (1998).
[13] A. A. Zakhidov, R. H. Baughman, Z. Iqbal, C. Cui, I. Khairulin, S. O. Dantas, J. Marti, and V. G. Ralchenko, Science **282**, 897 (1998).
[14] Yu. A. Vlasov, N. Yao, and D. J. Norris, Adv. Mater. **11**, 165 (1999).
[15] Yu. A. Vlasov, K. Luterova, I. Pelant, B. Hönerlage, and V. N. Astratov, Appl. Phys. Lett. **71**, 1616 (1997).
[16] W. Stöber, A. Fink, and E. Bohn, J. Colloid Interface Sci. **26**, 62 (1968).

[17] J. A. Valdmanis, R. L. Fork, and J. P. Gordon, Opt. Lett. **10**, 131 (1985).
[18] C. Hirlimann, O. Seddiki, J.-F. Morhange, R. Mounet, and A. Goddi, Opt. Commun. **59**, 52 (1986).
[19] S. Petit, O. Cégut, and C. Hirlimann, Opt. Commun. **124**, 49 (1996).
[20] See, for example, S. Datta, C. T. Chan, K. M. Ho, and C. M. Soukoulis, Phys. Rev. B **48**, 14 396 (1993).
[21] A. M. Steinberg, P. G. Kwiat, and R. Y. Chiao, Phys. Rev. Lett. **71**, 708 (1993).
[22] A. M. Steinberg and R. Y. Chiao, Phys. Rev. A **51**, 3525 (1995).
[23] R. L. Fork, C. H. Brito Cruz, P. C. Becker, and C. V. Shank, Opt. Lett. **12**, 483 (1987).
[24] K. W.-K. Shung and Y. C. Tsai, Phys. Rev. B **48**, 11 265 (1993).
[25] M. P. van Albada, B. A. van Tiggelen, A. Lagendijk, and A. Tip, Phys. Rev. Lett. **66**, 3132 (1991).
[26] G. H. Watson, P. A. Fleury, and S. L. McCall, Phys. Rev. Lett. **58**, 945 (1987).
[27] R. Garg, R. K. Prud'homme, I. K. Aksay, F. Liu, and R. R. Alfano, J. Opt. Soc. Am. A **15**, 932 (1998).
[28] Yu. A. Vlasov, M. A. Kaliteevski, and V. V. Nikolaev, Phys. Rev. B (to be published).
[29] S. John, Phys. Rev. Lett. **58**, 2059 (1987).